International Journal of Ethics in Engineering & Management Education
Website: www.ijeee.in (ISSN: 2348-4748, Volume 3, Issue 2, February 2016)

A Study on Surface Instabilities in Newtonian and Non-Newtonian Fluids

Shaik Kasimali
Research scholar
SunRise University-Alwar
kasimalishaik@gmail.com

Dr. Puneet Kumar
Director at GIER, Gzb
drkumarpuneet@gmail.com

Abstract: - **This paper on surface instability in Newtonian and non-Newtonian fluids. A first classification establishes fluids as compressible and incompressible, according to their response to an externally applied pressure. This paper is to introduce and to illustrate the frequent and wide occurrence of non-Newtonian fluid behavior in a diverse range of applications, both in nature and in technology. Representative examples of materials (foams, suspensions, polymer solutions and melts), which, under appropriate circumstances, display shear-thinning, shear-thickening, visco-plastic, time-dependent and visco-elastic behaviour are presented. Each type of non-Newtonian fluid behaviour has been illustrated via experimental data on real materials. This is followed by a short discussion on how to engineer non-Newtonian flow characteristics of a product for its satisfactory end use by manipulating its microstructure by controlling physico-chemical aspects of the system. Finally, we touch upon the ultimate question about the role of non-Newtonian characteristics on the analysis and modeling of the processes of pragmatic engineering significance.**

Key words:- **Non Newtonian fluids, Newtonian Fluids, Surface instability, shear-thinning, shear-thickening, visco-plastic, and visco-elastic behavior.**

1. INTRODUCTION

Most low molecular weight substances such as organic and inorganic liquids, solutions of low molecular weight inorganic salts, molten metal's and salts, and gases exhibit Newtonian flow characteristics, [5] i.e., at constant temperature and pressure, in simple shear, the shear stress (σ) is proportional to the rate of shear ($\gamma^{\cdot}$) and the constant of proportionality is the familiar dynamic viscosity (η). Such fluids are classically known as the Newtonian fluids, albeit the notion of flow and of viscosity predates Newton. For most liquids, the viscosity decreases with temperature and increases with pressure. For gases, it increases with both temperature and pressure. Broadly, higher is the viscosity of a substance, more resistance it presents to flow (and hence more difficult to pump). Table provides typical values of viscosity for scores of common fluids. As we go down in the table, the viscosity increases by several orders of magnitude, and thus one can argue that a solid can be treated as a fluid whose viscosity tends towards infinity, $\eta \rightarrow \infty$. Thus, the distinction between a fluid and a solid is not as sharp as we would like to think! Ever since the formulation of the equations of continuity (mass) and momentum (Cauchy, Navier-Stokes), the fluid dynamics of Newtonian fluids has come a long way during the past 300 or so years, albeit significant challenges especially in the field of turbulence and multi-phase flows still remain. The problem of thermal convection in fluids in porous medium is or considerable importance in geophysics, soil sciences, found water hydrology and astrophysics. The physical properties of comets, Meteorites and interplanetary dust strongly suggest the importance of porosity in astrophysical context [McDonnell (1978)]. The physics of flow through porous medium has been given in a [2] treatise by Scheidegger (1960). The Rayleigh instability of a thermal boundary layer in flow in porous medium is studied by Wooding (1960). Such problem arises in Oceanography, limnology and engineering. The idealization of uniform gravity assumed in theoretical investigations, although valid for laboratory purposes, can scarcely, be justified for large-scale convection phenomena occurring in atmosphere, the Ocean or mantle of the earth. It three becomes imperative to consider gravity as variable quantity varying with distance from surface or referee, print. G.K. Prndhan et, al (1989) studied the thermal instability of a fluid layer in a valuable gravitational field and found that variable gravity has destabilizing effect on the fluid layer. In the present paper an attempt has been Include to effect of variable gravity on the thermal instability or Maxwell visco-elastic fluid in porous mediums.

Formulation of Problem and Perturbation Equations

Consider an infinite horizontal layer of Maxwell Visco-elastic fluid of thickness „d" bounded by plane z = 0 and z = d in porous medium of porosity ε are medium permeability k1. The layer is heated from below such that a uniform temperature gradient $\beta = d$, where T is temperature. The system is acted upon by linear variable gravity force g 0,0,g z , where g(z) = g0 (1 + Mz) > 0, M is gravity parameter and g0 is the value of g at z = 0. Let p,,,,μ,υ and κ be the pressure, density, temperature and thermal coefficient of expansion. Viscosity, kinematic viscosity and thermal diffusivity of fluid respectively.

Non-Newtonian Fluid Behavior

The simplest possible deviation from the Newtonian fluid behavior occurs when the simple shear data $\sigma - \gamma^{\cdot}$ does not pass through the origin and/ or does not result into a linear relationship between σ and $\gamma^{\cdot}$. Conversely, the apparent viscosity, de- fined as $\sigma/\gamma^{\cdot}$, is not constant and is a function of σ or $\gamma^{\cdot}$. Indeed, under appropriate circumstances, the apparent

International Journal of Ethics in Engineering & Management Education
Website: www.ijeee.in (ISSN: 2348-4748, Volume 3, Issue 2, February 2016)

viscosity of certain materials is not only a function of flow conditions (geometry, rate of shear, etc.), but it also depends on the kinematic history of the fluid element under consideration. It is convenient, though arbitrary (and probably unscientific too), to group such materials into the following three categories:

1. Systems for which the value of $\dot{\gamma}$ at a point within the fluid is determined only by the current value of σ at that point; these substances are variously known as purely viscous, inelastic, time-independent or generalized Newtonian fluids (GNF).

2. Systems for which the relation between σ and $\dot{\gamma}$ shows further dependence on the duration of shearing and kinematic history; these are called time-dependent fluids, and finally.

3. Systems which exhibit a blend of viscous fluid behavior and of elastic solid-like behaviour. For instance, this class of materials shows partial elastic recovery, recoil, creep, etc. Accordingly, these are called visco-elastic or elastico-viscous fluids. As noted earlier, the aforementioned classification scheme is quite arbitrary, though convenient, because most real materials often display a combination of two or even all these types of features under appropriate circumstances. For instance, it is not uncommon for a polymer melt to show time-independent (shear-thinning) and visco-elastic behavior simultaneously and for a china clay suspension to exhibit a combination of time-independent (shear-thinning or shear-thickening) and time-dependent (thixotropic) features at certain concentrations and /or at appropriate shear rates. Generally, it is, however, possible to identify the dominant non Newtonian aspect and to use it as basis for the subsequent process calculations. Each type of non- Newtonian fluid behavior is now dealt with in more detail.

2. LITERATURE REVIEW

Kafoussias and Williams et.al (2014) studied, using an efficient numerical technique, the effect of a temperature-dependent viscosity on an incompressible fluid in steady, laminar, free-forced convective boundary layer flow over an isothermal vertical semi-infinite flat plate. Kozhhoukharova et al. (2014) examined the influence of a temperature-dependent viscosity on the axisymmetric steady thermo capillary flow and its stability with respect to non-axisymmetric perturbations by means of a linear stability analysis. Horne and Sullivan et.al (2014) examined the effect of temperature-dependent viscosity and thermal expansion coefficient on the natural convection of water through permeable formations. Richter et al. (2013) showed, by an experiment with temperature-dependent viscosity ratio as large as 106 , the existence of subcritical convection of finite amplitude near the critical Rayleigh number. Busse and Frick et.al (2013) analyzed the problem of RBC with linear variation of viscosity and showed an appearance of square pattern for a viscosity ratio larger than 2. Severin and Herwig et.al (2013) investigated the variable viscosity effect on the onset of instability in the RBC problem. Palm et.al (2012) showed that for a certain type of temperature-dependence of viscosity, the critical Rayleigh number and the critical wave number are smaller than those for constant viscosity and explained the observed fact that steady hexagonal cells are formed frequently at the onset of convection. Perez-Garcia and Carneiro (2012) analyzed the effects of surface tension and buoyancy on the convective instability in a layer of fluid with a deformable free surface. Their analysis is restricted to fixed values of a Prandtl number and Biot number in order to determine the role of the Crispation number on convection. Maxwell et.al (2011) had published the famous "velocity slip boundary condition".

Moffatt et.al (2010) first derived the value of the maximum amount of fluid a rotating cylinder can sustain. Brookfield Engineering Labs Inc. et.al (2010a) emphasized that by measuring the rheology parameters of fluids much useful behavioral and predictive information can be obtained. Brookfield engineering labs inc. et.al (2010a) defined that the viscosity is the measure of the internal friction of a fluid. Chhabra, et.al (2010) in practice, apparent viscosity in some fluids may depend on the rate of shear and also the time for which the fluid has been subjected to shearing. Gilbert et al (2010) proposed a three parameter to correlate the drag coefficient and the particle Reynolds number. Lauga & Stone et.al (2003) say „when the fluid does not completely wet an atomically smooth substrate, then might expect (even rarefied gases or liquids), or at least it has been conjectured, that the flow may exhibit expect, or at least it has been conjectured, that may exhibit some manifestations of microscopic slip". Hossain et al. (2002) analyzed the effect of temperature-dependent viscosity on natural convection flow from a vertical wavy surface using an implicit finite difference method. Takashima (2001, 2002) examined the effect of a free surface deformation on the onset of stationary and oscillatory surface tension driven instability using linear stability theory.

Time-Independent Fluid Behavior

As noted above, in simple unidirectional shear, this sub-set of fluids is characterized by the fact that the current value of the rate of shear at a point in the fluid is determined only by the corresponding current value of the shear stress and vice versa. Conversely, one can say that such fluids have no memory of their past history. Thus, their steady shear behavior may be described by a relation of the form,

$\gamma yx = f(\sigma yx)$

Or, its inverse form,

$\sigma yx = f -1 (\gamma yx)$

Depending upon the form of equation, three possibilities exist:

1. Shear- thinning or pseudo plastic behavior.
2. Visco-plastic behavior with or without shear-thinning behavior.
3. Shear- thickening or dilatant behavior.

International Journal of Ethics in Engineering & Management Education
Website: www.ijeee.in (ISSN: 2348-4748, Volume 3, Issue 2, February 2016)

Fig-1. shows qualitatively the flow curves (also called rheograms) on linear coordinates for the above- noted three categories of fluid behavior; the linear relation typical of Newtonian fluids is also included in Fig. Fig-1. Qualitative flow curves for different types of non Newtonian fluids.

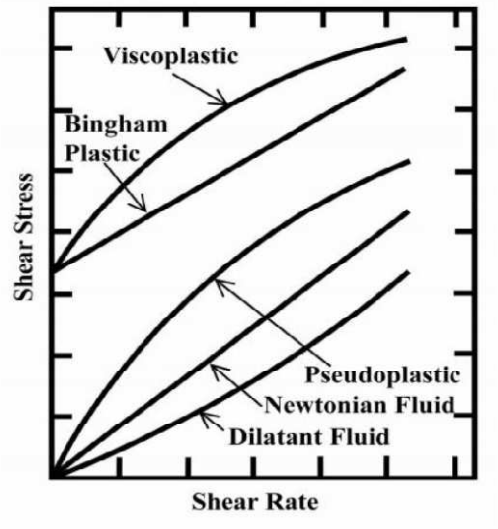

FIG-1: Shear rate vs Shear Stress

Shear-Thinning Fluids This is perhaps the most widely encountered type of time-independent non-Newtonian fluid behavior in engineering practice. It is characterized by an apparent viscosity η (defined as σyx/γ˙yx) which gradually decreases with increasing shear rate. In polymeric systems (melts and solutions), at low shear rates, the apparent viscosity approaches a Newtonian plateau where the viscosity is independent of shear rate (zero shear viscosity, η0).

$$\lim_{\dot{\gamma}_{yx}\to 0} \frac{\sigma_{yx}}{\dot{\gamma}_{yx}} = \eta_0$$

Furthermore, only polymer solutions also exhibit a similar plateau at very high shear rates (infinite shear viscosity, η∞), i.e.,

$$\lim_{\dot{\gamma}_{yx}\to \infty} \frac{\sigma_{yx}}{\dot{\gamma}_{yx}} = \eta_\infty$$

In most cases, the value of η∞ is only slightly higher than the solvent viscosity ηs . Fig. 5 shows this behavior in a polymer solution embracing the full spectrum of values going from η0 to η∞ . Obviously, the infinite-shear limit is not seen for polymer melts and blends, or foams or emulsions or suspensions. Thus, the apparent viscosity of a pseudoplastic substance decreases with the increasing shear rate, as shown in Fig. 6 for three polymer solutions where not only the values of η0 are seen to be different in each case, but the rate of decrease of viscosity with shear rate is also seen to vary from one system to another as well as with the shear rate interval considered. Lastly, the value of shear rate marking the onset of shear-thinning is influenced by several factors such as the nature and concentration of polymer, the nature of solvent, etc for polymer solutions and particle size shape, concentration of solids in suspensions, for instance. Therefore, it is impossible to suggest valid generalizations, but many polymeric systems exhibit the zero-shear viscosity region below $\dot{\gamma} < 10{-}2\ s\ {-}1$. Usually, the zero-shear viscosity region expands as the molecular weight of polymer falls, or its molecular weight distribution becomes narrower, or as the concentration of polymer in the solution is reduced.

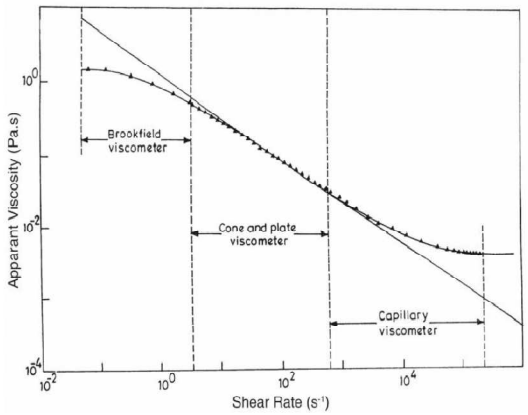

Fig-2. Demonstration of zero shear and infinite shear viscosities for a polymer solution

Power Law or Ostwald de Waele Equation

Often the relationship between shear stress (σ) − shear rate(γ˙) plotted on log-log co-ordinates for a shear-thinning fluid can be approximated by a straight line over an interval of shear rate, i.e.,

σ = m(γ˙)n
or, in terms of the apparent viscosity,
η = m(γ˙)n−1

Obviously, 0 < n < 1 will yield (dη/dγ˙) < 0, i.e., shear-thinning behaviour fluids are characterized by a value of n (power-law index) smaller than unity. Many polymer melts and solutions exhibit the value of n in the range 0.3-0.7 depending upon the concentration and molecular weight of the polymer, etc. Even smaller values of power-law index (n~0.1−0.15) are encountered with fine particle suspensions like kaolin-in-water, bentonite-in-water, etc. Naturally, smaller is the value of n, more shear-thinning is the material. The other constant, m, (consistency index) is a measure of the consistency of the substance. Although, eq. offers the simplest approximation of shear-thinning behaviour, it predicts neither the upper nor the lower Newtonian plateaus in the limits of $\dot{\gamma} \to 0$ or $\dot{\gamma} \to \infty$. Besides, the values of m and n are reasonably constant only over a narrow interval of shear rate range whence one needs to know a priori the likely range of shear rate to be encountered in an envisaged application.

International Journal of Ethics in Engineering & Management Education
Website: www.ijeee.in (ISSN: 2348-4748, Volume 3, Issue 2, February 2016)

3. EXPERIMENT SETUP AND TESTING METHOD

The experiment utilizes an adaptation of the filament stretching rheometer to implement a modification of the probe-tack adhesion test for the purpose of investigating endplate instabilities in mobile viscoelastic polymer solutions. The standard probe-tack test, which was discussed briefly in the last chapter, incorporates a flat probe that can be retracted from an adhesive substrate at a known rate while recording the maximum normal load. The current experiment deviates from the probe-tack test in the following ways:

1) Due to the mobile nature of the test fluids, a cylindrical sample having the same 5mm diameter as the probe is used rather than an infinite substrate of adhesive material;

2) The velocity profile is exponential in time, rather than the constant 10 mm/s back-off velocity specified by ASTM D2979-95. The aim of using an exponential velocity profile is to provide a constant strain rate within the elongating sample. This is a fundamental requirement in extensional rheometry and in the current case, it is required in order to induce a strongly strain hardening elastic response in the viscoelastic test fluids;

3) The test probe material is glass rather than the polished stainless steel called for by the standard. This is because the implementation of the optical device for viewing the sample from beneath the endplate required that a transparent material be used for the lower endplate. A matching glass optical window was used for the upper endplate to ensure flow symmetry at low plate separation distances and to provide symmetrical conditions for the occurrence of adhesive failure at the end of stretching. The fluid sample is initially in the shape of a cylindrical plug and is held between two rigid circular endplates by surface tension. The upper endplate is attached to the linear motor, and can move away from the stationary and mechanically isolated lower endplate at a programmable rate. At the start of an experiment the plates begin to separate, thus deforming the fluid sample. Depending upon the initial experiment parameters, a slender fluid filament may form. If a stable filament does develop, then the flow near the filament midpoint will be a nearly pure uniaxial extensional flow if an exponential profile is chosen. This shearfree flow is the key the success of filament stretching rheometry.

4. EXPERIMENTAL CONDITIONS

The experiments were conducted in a 26-m long, 0.6-m wide and 0.5-m high tilting flume with glass sided walls. The original channel bed was made of steel plate and was hydraulically smooth even for flow of water and the bed slope can be adjusted in the range 0-0.05. Clay suspensions were recalculated through the channel. The flow rate was controlled by means of an inlet valve and measured by using a magnetic flow meter. For supercritical flow of Froude number larger than one, the tailgate was open al-lowing How out off freely. For subcritical How, the flow depths were adjusted by means of an overflow weir at the downstream end of the channel to achieve uniform flow conditions. The water depth was measured by using scaling arrow with digital readout to within 0.1mm at worst. Except for a few experiment the depth of the How was in a range from 1 to 12 cm. which yielded width to depth ratios larger than 5:1. so that the How was effectively two dimensional and five from wall effects in the central zone of the channel.

The clay material has a density of 2.68 g/cm3 and median diameter of 0.002 mm. The main mineral compositions were montmorillonite, quartz and calcite. Clay and tap water was well mixed and the suspensions behaved like a viscous liquid rather than solid water mixture. Clay concentrations of the samples were analysed by using picnometer. The measurement error of concentration was 0.0004. The 109
pH value of the suspensions. The rheologic behavior of the suspensions was studied with a rotating coaxial cylinder viscometer (Wang. Larsen and Xiang, 1994). Samples of clay suspensions were taken from the flume and tested with the viscometer. For concentrations of less than 1.6%, the suspension exhibits very small yield stress and can be regarded still Newtonian but with high viscosity. For higher concentrations, it showed obvious yield stress and roughly followed the Bingham theological model given by Eq. The temperature of water and clay suspensions was maintained in the range 19-220C for all experiments. The effect of the variation in temperature on the theological properties was negligible in which τBm=12000 Pa and (a is the viscosity of clear water, Cv is the volume concentration of clay. A video camera and a sounding meter were used to record the development of the waves. The velocity was measured by using a one component pressure veloeimeter. The tip of the sensor is 1 mm in diameter. The probe size, working principle, calibration and relative error of measurement are presented in a literature (Wang el al., 1995). The veloeimeter can measure turbulence with sampling frequency 300 Hz. All the flows were laminar because the clay suspensions were high viscous.

5. EFFECTS OF SURFACE TENSION ON THE STABILITY OF TWO SUPERPOSED NEWTONIAN FLUIDS

This chapter deals with the effects of surface tension on she instability of the interface separating two superposed Newtonian fluids immersed in a two dimensional horizontal magnetic field. Employing the normal mode technique the linearized perturbation equations have been solved and the dispersion relation has been derived. For several values of the physical parameters involved, the dispersion relation has been solved numerically and it found that the surface tension newtonian and non-newtonain all suppress the Instability of i/se system. A detailed account of the various investigation in hydrodynamics and Hydromagnetics of the Rayleigh Taylor insatiability, which arises from the character or the equilibrium or a layer of a heterogeneous fluid and or which the two superposed lasers of homogeneous fluids is a particular case has been given by Chandrasekhar. Bhatia has

International Journal of Ethics in Engineering & Management Education
Website: www.ijeee.in (ISSN: 2348-4748, Volume 3, Issue 2, February 2016)

studied the Rayleigh-Taylor instability of two Superposed electrically conducting viscous fluids in a horizontal magnetic field. Rayleigh-Taylor instability has been studied by several researchers under varying aspects. Bhatia and Chhonkar have studied the stability or superposed viscous rotating plasma m the presence or finite Larmor Radius (FLR) effects while Hooper and Grimshaw have examined the nonlinear instability of the interface between two fluids Gupta and Bhatia have studied the stability of plane interface between two viscous superposed partially ionized plasmas of uniform densities in a uniform two dimensional horizontal magnetic Filed Srivastava and Khare have Investigated the Rayleigh-Taylor instability of two viscous superposed conducting fluids in a vertical magnetic field, Osorozco has studied the Rayleigh-Taylor instability of a two fluid layer under a general rotational field and a horizontal magnetic field Allah IMI has investigated the effects of surface tension and heat and mass transfer on the instability of two steaming superposed fluids. All the above investigations have been carried out for the Newtonian fluids. Since visco-elastic fluids play an important role in industrial applications. Sharma and Kumar have studied the Rayleigh-Taylor instability of two superposed conducting Walter‟s B‟ etastico-viscous fluids in 2-D magnetic field, Recently Kitan and Bhatia 1101 have stndied the stability of two superposed visco-elastic fluids through porous medium. In both these studies the effect of surface tension has not been included As the forces arising form surface tension where the density changes discontinuously play an important role, it would therefore be of interest to investigate the effects of surface tension on the Rayleigh-Taylor instability of two superposed conducting Walters B‟ newtonian fluids This aspect forms the basis of this paper where in the fluids are permeated by n uniform two dimensional horizontal magnetic field .We have carried out the stability analysis for two fluids of equal kinematic newtonian and non-newtonian but different densities.

Formulation of The Problem And Perturbation Equations

We consider the motion or an incompressible infinitely conducting Walters BrcIastico-visc0us fluid of enable density The fluid is assumed to be immersed in a uniform magnetic field *(H.H.O) and* is arranged in horizontal strata The relevant lineanzed perturbation equations are

$$\rho\frac{\partial\vec{v}}{\partial t}=-\nabla\delta p+\vec{g}\delta\rho+\rho\left(\gamma-\gamma'\frac{\partial}{\partial t}\right)\nabla^2\vec{v}+\frac{1}{4\pi}(\nabla\times\vec{h})\times\vec{H}$$

$$+\left(\frac{d\mu}{dz}-\frac{\partial}{\partial t}\frac{d\mu'}{dz}\right)\left(\frac{\partial w}{\partial\vec{x}}+\frac{\partial\vec{v}}{\partial z}\right)+\sum_s\left[T_s\left(\frac{\partial^2}{\partial x^2}+\frac{\partial^2}{\partial y^2}\right)\delta z_s\right](z-z_s),$$

$$\nabla\cdot\vec{v}=0$$

$$\nabla\cdot\vec{h}=0$$

$$\frac{\partial}{\partial t}\delta\rho=-wD\rho$$

$$\frac{\partial}{\partial t}\delta z_s=w_s$$

$$\frac{\partial\vec{h}}{\partial t}=\nabla\times\left(\vec{v}\times\vec{H}\right)$$

Where

$$\vec{v}(u,v,w),\delta\rho,\delta p\quad\&\quad\vec{h}(h_x,h_y,h_z)$$

denote the perturbations in velocity density ρ presume p. and magnetic field H respectively Here T, μ,′ and g = (0, 0, -g) arc respectively the surface tension, co-efficient of viscosity, coefficient of visco elasticity and acceleration due to gravity In above equations $\delta(z-zs)$ denotes Dirac‟s δ function, x = (x, y, z) and $D = d/dz$ Equation ensures that the density of ever panicle remains unchanged as we follow it with its motion. Analyzing in terms of normal modes, we assume that the perturbed quantities have the space *(x, y, z)* and time (t) dependence of the form

$$f(z)\exp(ik_x x+ik_y y+nt),$$

Where f(z) is some function *of z, k* and *k,,* are the horizontal numbers (k2 = *k2x* + *k2x)* and *n* is the growth rate of harmonic disturbance. For the perturbation of the form equations become

$$\rho nu=-ik_x\delta p+\rho(\gamma-n\gamma')(D^2-k^2)\ u+\frac{H_y}{4\pi}(ik_yh_x-ik_xh_y)+$$
$$(D\mu-nD\mu')(ik_xw+Du)$$

$$\rho nv=-ik_y\delta p+\rho(\gamma-n\gamma')(D^2-k^2)\ v+\frac{H_x}{4\pi}(ik_xh_y-ik_yh_x)+$$
$$(D\mu-nD\mu')(ik_yw+Dv)$$

$$\rho nw=-D\delta p-g\delta\rho+\rho(\gamma-n\gamma')(D^2-k^2)\ w+\frac{H_x}{4\pi}(ik_xh_x-Dh_x)$$
$$+\frac{H_y}{4\pi}(ik_yh_z-Dh_y)+2(D\mu-nD\mu')Dw-\frac{k^2T}{n}\delta(z-z_s)w$$

$$ik_xu+ik_yv+Dw=0$$

$$ik_xh_x+ik_yh_y+Dh_z=0$$

$$\delta\rho=-wD\rho$$

$$n\vec{h}=(ik_xH_x+ik_yH_y)\ \vec{v}$$

Eliminating some of the variables from the above equations. Obtain following equation in

International Journal of Ethics in Engineering & Management Education
Website: www.ijeee.in (ISSN: 2348-4748, Volume 3, Issue 2, February 2016)

$$n\left[D(\rho Dw)-k^2\rho w\right]+\frac{gk^2}{n}(D\rho)w-\left[D\left\{\rho(\gamma-\gamma' n)(D^2-k^2)Dw\right\}\right]$$
$$-k^2\rho(\gamma-\gamma' n)(D^2-k^2)w+\frac{1}{4\pi n}(k_xH_x+k_yH_y)^2(D^2-k^2)^2w$$
$$-\left[D\left\{(D\mu-nD\mu')(D^2-k^2)^2w\right\}-2k^2(D\mu-nD\mu')Dw\right]$$
$$+\frac{k^4T}{n}\delta(z-z_s)w=0$$

This equation holds for a fluid in which density ρ, viscosity μ and viscoclasticity μ'.

Two Superposed Walters B' Fluids Separated *By* a Horizontal, Boundary Consider now the case when two superposed Walters B ‟ fluids of unfound densities ρ and ρ' , uniform viscosities μ and $\mu 2$ and uniform viscoelastictics p, and occupy the regions $z < 0$ and $z > 0$ and are separated b a horizontal boundary at $z = 0$. Therefore in both regions $z < 0$ and $z > 0$ are equation becomes

$$(D^2-k^2)(D^2-q^2)w=0$$

$$q^2=k^2+\frac{n}{\gamma-n\gamma'}\left[1+\frac{1}{4\pi n^2\rho}(k_xH_x+k_yH_y)^2\right]$$

we can write the solutions of equation appropriate to the two regions, as

$$w_1 = A_1e^{+kz} + B_1e^{+q_1z} \qquad (z<0)$$

$$w_2 = A_2e^{-kz} + B_2e^{-q_2z} \qquad (z>0)$$

where *A1 B1,. A2, B2* arc constants of integration, and q1 and q2 arc the positive square roots of equation for the two regions. It is assumed here that q1 and q2 are so defined that their real parts arc positive.

Boundary Conditions

The solutions must satisfy four boundary conditions. The three conditions to be satisfied at the interface $z = 0$ are that

$$w\ ,\ Dw\ ,\ (\mu-\mu' n)(D^2+k^2)\ w$$

must be Continuous. If we integrate equation across the interface, we obtain the required fourth condition as

$$\left[\rho_2Dw_2-\rho_1Dw_1\right]_{z=0}-\left[\frac{1}{n}\left(\mu_2-n\mu_2'\right)(D^2-k^2)Dw_2-\frac{1}{n}\left(\mu_1-n\mu_1'\right)(D^2-k^2)Dw_1\right]_{z=0}$$
$$+\frac{(k_xH_x+k_yH_y)^2}{4\pi n^2}(Dw_2-Dw_1)_{z=0}=\frac{k^4T}{n^2}w_0-\frac{gk^2}{n}(\rho_2-\rho_1)w_0$$
$$-\frac{2k^2}{n}\left(\mu_2-n\mu_2'-\mu_1+n\mu_1'\right)(Dw)_0$$

where w0 and *(Dw)0* are unique values of these quantities at $z = 0$ On applying the conditions to the solutions, we obtain four relations in *A1, B1, A2* and *B2,*

$$A_1 + B_1 = A_2 + B_2$$
$$kA_1 + q_1B_1 = -kA_2 - q_2B_2$$
$$(\mu_1-n\mu_1')\left[2k^2A_1+(q_1^2+k^2)B_1\right]=(\mu_2-n\mu_2')\left[2k^2A_2+(q_2^2+k^2)B_2\right]$$
$$\left[-k\rho_2A_2-kq_2A_2-k\rho_1A_1-kq_1A_1\right]-\left[\begin{matrix}\frac{1}{n}(\mu_2-n\mu_2')(-q_2)(q_2^2-k^2)B_2\\ -\frac{1}{n}(\mu_1-n\mu_1')(-q_1)(q_1^2-k^2)B_1\end{matrix}\right]+$$
$$\left[-kA_2-q_2B_2-kA_1-q_1B_1\right]\frac{(k_xH_x+k_yH_y)^2}{4\pi n^2}+\frac{gk^2}{2n^2}\left\{(\rho_2-\rho_1)-\frac{k^2T}{g}\right\}\times$$
$$(A_1+B_1+A_2+B_2)+\frac{k^2}{n}(\mu_2-n\mu_2'-\mu_1+n\mu')(kA_1+q_1B_1-kA_2-q_2B_2)=0$$

On eliminating the constants A1, B1, A2, B2 and evaluating the determinate of the given matrix of the coefficients in equations we obtain characteristic equation

$$(q_1-k)\left[-2k^2C\left\{-\frac{k}{n}C(q_2-k)+\alpha_2+\frac{(\vec{k}\vec{V}_A)^2}{n^2}\right\}+\left\{R+S-1-\frac{2(\vec{k}\vec{V}_A)^2}{n^2}\right\}\times(\gamma_2\alpha_2-n\gamma_2'\alpha_2)(q_2^2-k^2)\right]$$
$$-2k\left[(\gamma_1\alpha_1-n\gamma_1'\alpha_1)(q_1^2-k^2)\times\left\{-\frac{k}{n}C(q_2-k)+\alpha_2+\frac{(\vec{k}\vec{V}_A)^2}{n^2}\right\}\right](\gamma_2\alpha_2-n\gamma_2'\alpha_2)(q_2^2-k^2)$$
$$\times\left\{\frac{k}{n}C(q_1-k)+\alpha_1+\frac{(\vec{k}\vec{V}_A)^2}{n^2}\right\}+(q_2-k)\left[\begin{matrix}(\gamma_1\alpha_1+n\gamma_1'\alpha_1)(q_1^2-k^2)\times\left\{R+S-1-\frac{2(\vec{k}\vec{V}_A)^2}{n^2}\right\}+2k^2C\times\\ \left\{+\frac{k}{n}C(q_2-k)+\alpha_1+\frac{(\vec{k}\vec{V}_A)^2}{n^2}\right\}\end{matrix}\right]=0$$

$$(\vec{k}.\vec{V}_A)^2=\frac{(k_xH_x+k_yH_y)^2}{4\pi(\rho_1+\rho_2)}=\frac{k^2(H_x\cos\theta+H_y\sin\theta)^2}{4\pi(\rho_1+\rho_2)}$$

$$S=\frac{k^3T}{n^2}\quad,\quad R=\frac{gk}{n^2}(\alpha_2-\alpha_1)$$

$$C=(\gamma_2\alpha_2-n\gamma_2'\alpha_2-\gamma_1\alpha_1+n\gamma_1'\alpha_1)$$

$$\alpha_{1,2}=\frac{\rho_{1,2}}{\rho_1+\rho_2}$$

$$\gamma_{1,.2}=\frac{\mu_{1,2}}{\rho_{1,2}}\quad,\quad\gamma_{1,2}'=\frac{\mu_{1,2}'}{\rho_{1,2}}$$

$\vec{V}_A$ being Alfven velocity vector θ being angle which k makes with K-axis. The dispersion relation is quite complex, particularly as q1 and q2, involve square roots. We, therefore can out the stability anal‟ sis for large viscosity and large viscoclasticity for then we can write q1 and q2 as

$$q_{1,2}-k=\left[\frac{n}{2(\gamma_{1,2}-n\gamma_{1,2}')k}\left\{1+\frac{(\vec{k}\vec{V}_{A_{1,2}})^2}{\alpha_{1,2}n^2}\right\}\right]$$

Substituting the values of q1 and q2, we get the dispersion relation which involves the values of the parameters α, γ, γ' , $V\ A$. corresponding to two fluids. As we wish to obtain

International Journal of Ethics in Engineering & Management Education
Website: www.ijeee.in (ISSN: 2348-4748, Volume 3, Issue 2, February 2016)

qualitatively the influence of these effects on the instability of the system we set $\gamma 1 = \gamma 2 = \gamma$, $\gamma 1' = \gamma 2' = \gamma'$

$\vec{V}_A = \vec{V}_{A2} = \vec{V}_A$ For the mathematical simplicity. The dispersion relation is then,

$$\left[\alpha_1\alpha_2\left(1-2k^2\gamma'\right)\right]n^6+\left[2k^2\alpha_1\alpha_2\gamma\right]n^5+\left[\alpha_1\alpha_2\left\{2\left(\vec{k}.\vec{V}_A\right)^2-gk\left(\alpha_2-\alpha_1\right)+K^3T\right\}+\left(\vec{k}.\vec{V}_A\right)^2\left(1-2k^2\gamma'\right)\right]n^4$$

$$+\left[2k^2\gamma\left(\vec{k}.\vec{V}_A\right)^2\right]n^3+\left[\left(\vec{k}.\vec{V}_A\right)^2\left\{2\left(\vec{k}.\vec{V}_A\right)^2-gk\left(\alpha_2-\alpha_1\right)+K^3T\right\}+\left(\vec{k}.\vec{V}_A\right)^4\left(1-2k^2\gamma'\right)\right]n^2$$

$$+\left[2k^2\gamma\left(\vec{k}.\vec{V}_A\right)^4\right]n+\left(\vec{k}.\vec{V}_A\right)^4\left[2\left(\vec{k}.\vec{V}_A\right)^2-gk\left(\alpha_2-\alpha_1\right)+k^3T\right]=0 \quad \ldots(1)$$

In the absence of the surface tension (T = 0), we recover the dispersion relation obtained earlier by Sharma and Kumar and if γ' is also zero, we obtain the dispersion relation derived by Bhatia.

6. DISCUSSION

The equation is quite complex In order to studs the *effects* of arouse physical parameters on the growth rate or unstable modes, the numerical solutions of this equation have been sought to locate the values or *n* (positive real part) against wave number k. for several values of the parameters involved The numerical calculations are presented in figures. where we have taken a potentially unstable arrangement b taking α1 = 0.25, α2 = 0.75 for fixed VA = 0.5, $\theta = 450$, $\alpha 2 > \alpha 1$

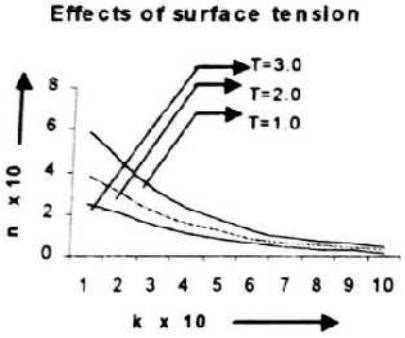

Fig-3: effects of surface tension

Variation of the growth rate *n* (positive real part) against the wave number *k* for different values of surface tension T taking α1 = 0.25, α2 = 0.75 & γ = 3.0, γ'=0.2, VA = 0.5, $\theta = 450$, Figure

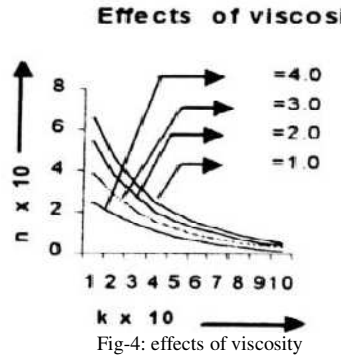

Fig-4: effects of viscosity

Variation of the growth rate *n* (positive real part) against the wave number *k* for different values or viscosity r taking α1 = 0.25, α2 = 0.75 & *T* = 4.0, γ'=0.2, VA = 0.5, $\theta = 450$ Figure.

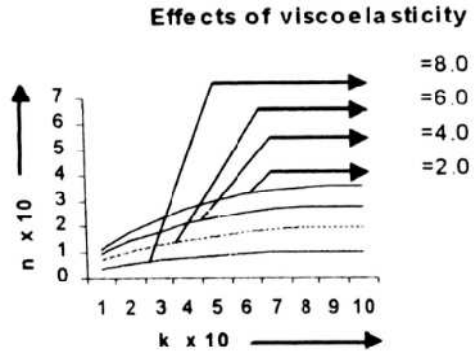

Fig-5: effects of viscoelasticity

Variation of the growth rate *n* (positive real part) against the wave number *k* for different values of newtonian (y") taking α1 = 0.25, α2 = 0.75 & γ = 3.0, *T*=4.0 VA = 0.5, $\theta = 450$ Figure. It is seen from the about figures that the growth rate n decreases as (surface tension), γ (kriematic visco-elasticity) and γ' (kinematic visco-elasticity) increase of *the* same k showing thereby the character of these effects. The findings are in agreement with the Instigations done earlier. We may thus cm dude that the surface tension as well as Newtonian and non-Newtonian all suppress the instability of the system.

7. CONCLUSIONS

Non-Newtonian laminar flow exhibits free surface instability, such as the river clogging in the hyper-concentrated flows, intermittent viscous debris flows and fluctuation in mudflows. Theoretical analysis from the equation of motion incorporating the non-Newtonian nature of the fluid demonstrated that the free surface instability is essentially caused by the yield stress. Two dimensionless numbers, Sy and Syis, representing the effects of yield stress and viscosity are calculated and compared for various flows. The free surface is unstable and roll waves may develop even at constant incoming flow rate if S is much larger than Syis and is stable if Sy is smaller than Syis Experiments show that river clogging occurs if the driving shear stress is nearly equal to the yield stress, a perturbation wave may grow up in non-Newtonian laminar flow if Sy is large, and a series of roll waves may develop if Sy is even larger. The experimental results agree well with the theoretical formula showing exponential law of growth of wave height. The growth rate of wave height depends essentially on the parameter SN. The larger is the parameter Sy the higher is the growth rate and the higher are the waves. The effect of the solid layer deformability on the free surface instability in liquid film flow down an inclined plane lined with a soft solid layer was analyzed first using a long wave asymptotic analysis, and then using a numerical solution of the governing stability equations. In the absence of the soft solid layer, the liquid film flow undergoes long wave instability due

International Journal of Ethics in Engineering & Management Education
Website: www.ijeee.in (ISSN: 2348-4748, Volume 3, Issue 2, February 2016)

to fluid inertia. The present asymptotic results show that the effect of the solid layer appears at the same order [O (k)] as the destabilizing effect of fluid inertia, but the deformability of the solid layer always has a stabilizing effect on the free-surface instability in the long-wave limit. Physically, at leading order in the asymptotic analysis, the normal and tangential fluid velocity fields satisfy the no slip condition as in a rigid inclined plane, and so the leading-order wave speed c (0) remains the same as in a rigid inclined plane. However, the leading-order fluid velocity field exerts a tangential stress on the solid layer, causing a deformation in the solid. This leading-order deformation in the solid layer affects the first correction to the fluid velocity field, thereby qualitatively altering the nature of the free surface instability. For a fixed value of Re and the inclination angle β, the free-surface instability is stabilized when =Vaη/(GR) increases beyond a critical value. The long wave asymptotic results are further extended to finite wavelengths using a numerical solution of the stability equations. In general, this shows that the suppression of the free-surface instability continues to finite wavelengths. However, an increase in Γ substantially away from the value required for stabilization of the free-surface instability results in destabilization of either the liquid-solid interfacial mode or the free surface interfacial mode at finite wavelengths. Representative numerical results presented for a variety of parameter regimes indicate, nevertheless, that there exists a wide range of values of typically two orders of magnitude where both the interfacial modes are stabilized at all wave numbers. Furthermore, the suppression of instability for all wavelengths is found to be valid only for Re~O(1); when the Reynolds number is increased to 10 (for = σ/ 4, it was found that there was always a finite-wavelength instability induced by the deformable solid layer. There are several implications from the present study for future experimental investigations. First, as discussed, the predicted stabilization can be realized in experiments involving the flow of viscous liquids viscosity1 − 10 Pa s past a soft elastomeric solid layer shear modulus104 Pa. Secondly, by decreasing the angle of inclination, it is possible to verify the destabilizing effect of solid layer deformability on the free-surface instability at finite wavelengths, when there is no long-wave instability in liquid flow down a rigid inclined plane. Thirdly, while the present study was restricted to the realm of linear stability, the nonlinear dynamics of liquid flow past an inclined plane lined with a soft solid layer could also potentially be qualitatively different from that of a rigid inclined plane. For example, it might be expected that the nonlinear evolution of the finite wavelength instability due to the deformability of the solid layer could be very different from that of the long-wave instability of liquid flow down a rigid inclined plate. This is an issue that is worth studying in future experimental and theoretical investigations. In conclusion, the present study predicts a discernible consequence of the elasto hydrodynamic coupling between the liquid flow and the deformation in the soft solid on the free-surface instability of falling liquid films which can be readily tested by experiments.

The filament stretching apparatus built by Anna has been modified in order to test mobile fluids in a manner quite similar to the probe-tack test used to test pressure-sensitive adhesives. The resulting experiment permits a very thin layer of a test fluid to be stretched at a preprogrammed rate while measuring the axial force as a function of time, or strain. In addition, a special endplate setup allows the fluid sample to be viewed from beneath and images are recorded with CCD camera. The dynamic response times of the linear motor and the force transducer were characterized experimentally. It was found that when these transient effects were accounted for in the measured experimental force data, the data matched the theoretical prediction of the Reynolds lubrication theory very well. It is concluded that the apparatus is well suited for the measurements undertaken in this thesis. The current experiments are intended to investigate flow instabilities that occur during stretching, and for these experiments, three model fluids were chosen.

REFERENCES

[1]. Moffatt, H. K. (2010) Behaviour of a viscous film on the outer surface of a rotating cylinder. Journal de mecanique, 16(5), 651-673.
[2]. O″Brien, S.B.G., Gath, E.G. (2011) Location of a shock in rimming flow. Physics of Fluids, 10, 1040-1042.
[3]. Bird, R. B., Armstrong, R. C., & Hassager, O. (2011) Dynamics of polymeric liquids. Vol. 1: Fluid mechanics.
[4]. Fomin, S., Watterson, J., Raghunathan, S., & Harkin-Jones, E. (2012) Steady-State Rimming Flow of the Generalized Newtonian Fluid, Physics of Fluids, 14(9), 3350-3353.
[5]. Rajagopalan, D., Phillips, R. J., Armstrong, R. C., Brown, R. A., & Bose, A. (2012) The influence of viscoelasticity on the existence of steady solutions in two-dimensional rimming flow. Journal of Fluid Mechanics, 235, 611-642.
[6]. Leslie, G. A., Wilson, S. K., & Duffy, B. R. (2013) Three-dimensional coating and rimming flow: a ring of fluid on a rotating horizontal cylinder. Journal of Fluid Mechanics, 716, 51-82.
[7]. Brookfield Engineering Labs Inc. 2010a. More Solutions to Sticky Problems: A Guide to Getting More from Your Brookfield Viscometer. Bull. Brookfield Eng. Labs, pp 1-53.
[8]. Chhabra, R.P. & Richardson, J.F. 2008). Non-Newtonian Flow and Applied Rheology. 2nd ed., Butterworth Heinemann, Oxford, UK.
[9]. Edil, T.B. & Wang, X. 2000. Shear Strength and K0 of Peats and Organic Soils. Geotechnics of high water content materials, ASTM STP 1374, West Conshohocken, Pa., USA, pp 209-225.
[10]. Amadei, B. & Savage, W.Z. 2001. An Analytical Solution for Transient Flow of Bingham Viscoplastic Materials in Rock Fractures. Int. J. Rock Mech, & Min. Sci., Vol. 38, pp 285-296.
[11]. Bird, R.B., Armstrong, R.C. & Hassager, O. 1987. Dynamics of Polymeric Liquids. Fluid Dynamics. 2nd ed., Vol. 1, Wiley Interscience, New York, USA.
[12]. Brookfield Engineering Labs Inc. 2008. Viscometers, Rheometers & Texture Analyzers for Laboratory and Process Applications. Brookfield Eng. Labs, pp 4-35.
[13]. Aul RW, OlbrichtWL. 1990. Stability of a thin annular film in pressure-driven, low-Reynolds-number flow through a capillary. *J. Fluid Mech.* 215:585–99
[14]. Azaiez J, Homsy GM. 1994. Linear stability of free shear flow of viscoelastic liquids. *J. FluidMech.* 268:31–69
[15]. Bai R, Chen K, Joseph DD. 1992. Lubricated pipelining: stability of core annular flow. Part 5. Experiments and comparison with theory. *J. Fluid Mech.* 240:97–132
[16]. Barthelet P, Charru F, Fabre J. 1995. Experimental study of interfacial long waves in a two-layer shear flow. *J. Fluid Mech.* 303:23–53

[17]. Bridgman PW. 1926. The effect of pressure on the viscosity of forty-three pure liquids. *Proc. Am. Acad.*61:57–99
[18]. Cao Q, Ventresca L, Sreenivas KR, Prasad AK. 2003. Instability due to viscosity stratification downstream of a centreline injector. *Can. J. Chem. Eng*. 81:913–22
[19]. Charles ME, Lilleleht LU. 1965. An experimental investigation of stability and interfacial waves in co-current flow of two liquids. *J. Fluid Mech.* 22:217–24
[20]. Charru F, Hinch EJ. 2000. 'Phase diagram' of interfacial instabilities in a two-layer Couette flow and mechanism for the long-wave instability. *J. Fluid Mech.* 414:195–223
[21]. Chekila A, Nouar C, Plaut E, Nemdili A. 2011. Subcritical bifurcation of shear-thinning plane Poiseuille flows. *J. Fluid Mech.* 686:272–98
[22]. Chen K, Bai R, Joseph DD. 1990. Lubricated pipelining. Part 3: stability of core-annular flow in vertical pipes. *J. Fluid Mech.* 214:251–86
[23]. Craik ADD. 1969. The stability of plane Couette flow with viscosity stratification. *J. Fluid Mech*. 36:685–93
[24]. Drazin PG, ReidWH. 1985. *Hydrodynamic Stability*. Cambridge, UK: Cambridge Univ. Press Ern P, Charru F, Luchini P. 2003. Stability analysis of a shear flow with strongly stratified viscosity. *J. Fluid Mech*. 496:295–312
[25]. Fjortoft R. 1950. Application of integral theorems in deriving criteria of stability for laminar flows and for the baroclinic circular vortex. *Geofys. Publ. Oslo* 17(6):1–52
[26]. Frenkel AL, Halpem D. 2002. Stokes-flow instability due to interfacial surfactant. *Phys. Fluids* 14:L45–48
[27]. Friederich T, Kloker MJ. 2012. Control of the secondary cross-flow instability using localized suction. *J. Fluid Mech.* 707:470–95
[28]. Frigaard I, Nouar C. 2003. On three-dimensional linear stability of Poiseuille flow of Bingham fluids. *Phys. Fluids* 15:2843–51
[29]. Frigaard IA. 2001. Super-stable parallel flows of multiple visco-plastic fluids. *J. Non-Newton. Fluid Mech.* 100:49–76
[30]. Fukui K, Asakuma Y, Maeda K. 2010. Determination of liquid viscosity at high pressure by DLS. *J. Phys. Conf. Ser.* 215:012073
[31]. Govindarajan R. 2004. Effect of miscibility on the linear instability of two-fluid channel flow. *Int. J. Multiphase Flow* 30:1177–92
[32]. Govindarajan R, L'vov SV, Procaccia I. 2001. Retardation of the onset of turbulence by minor viscosity contrasts. *Phys. Rev. Lett.* 87:174501
[33]. Goyal N,Meiburg E. 2006. Miscible displacements in Hele-Shaw cells: two-dimensional base states and their linear stability. *J. Fluid Mech.* 558:329–55
[34]. Guillot F, Colin A, Utada AS, Ajdari A. 2007. Stability of a jet in confined pressure-driven biphasic flows at low Reynolds number. *Phys. Rev. Lett.* 99:104502
[35]. Helfrich K. 1995. Thermo-viscous fingering of flow in a thin gap: amodel ofmagma flow in dikes and fissures. *J. Fluid Mech.* 305:219–38
[36]. Hickox CE. 1971. Instability due to viscosity and density stratification in axisymmetric pipe flow. *Phys. Fluids*
[37]. Coussot P (2005) Rheometry of pastes, suspensions and granular materials.Wiley, New York.
[38]. Dullaert K,Mewis J (2005) Thixotropy: Build-up and breakdown curves during flow. J Rheol49: 1213-1230.
[39]. Goodwin JW, Hughes RW (2008) Rheology for chemists: an introduction. The royal societyof chemistry, Cambridge.
[40]. Kroger M(2004) Simple models for complex non-equilibrium fluids. Phy. Rep. 390: 453-551.
[41]. Kroger M(2004) Simple models for complex non-equilibrium fluids. Phy. Rep. 390: 453-551.
[42]. Uhlherr PHT, Guo J, Zhang XM, Zhou JZQ, Tiu C (2005) The shear-induced solid-liquid transition in yield stress materials with chemically different structures. J Non-Newt Fluid Mech 125:101-119.